Transactions of the Materials Research Society of Japan 29[5] 2183-2186 (2004)

Nanoporous Glass by Pseudomorphic Transformation of Zeolite

Junichi Minato[1], Yujiro Watanabe[2], Keisuke Fukushi[3], Kenji Tamura[1] and Hirohisa Yamada[1*]

[1]National Institute for Materials Science, 1-1 Namiki, Tsukuba, Ibaraki 305-0044, Japan
Fax: 81-29-860-4667, e-mail: MINATO.Junichi@nims.go.jp, TAMURA.Kenji@nims.go.jp, YAMADA.Hirohisa@nims.go.jp

[2]Faculty of Engineering, Hosei University, 3-7-2 Kajino-cho, Koganei-shi, Tokyo 184-8584, Japan
Fax: 81-29-860-4667, e-mail: WATANABE.Yujiro@nims.go.jp

[3]National Institute of Advanced Industrial Science and Technology, 1-1-1 Higashi, Tsukuba, Ibaraki 305-8567, Japan
Fax: 81-29-861-3663, e-mail: fukushi.keisuke@aist.go.jp

*Correspondence: Hirohisa Yamada, National Institute for Materials Science

LTA type zeolite with Na ions (NaA zeolite) was treated with 0.06 M HCl for 10 min and hydrothermal treatments at 150 °C for 24 hours. The products were characterized by XRD, SEM with EDS, FT-IR, TG-DTA, and nitrogen adsorption measurement. The results showed that the noncrystalline pseudomorphism occurred due to the sodium-hydrogen ion exchange and subsequent reaction of the NaA zeolite framework with the incorporated H ion. TG-DTA and nitrogen adsorption measurements suggested that additional pores with mean diameter at 1.9 nm were formed during the subsequent hydrothermal treatment. The obtained glass with nanopores by pseudomorphic transformation may be useful for eco-functional materials such as adsorbents, catalysts, ion-exchange media, and membranes.

Key words: LTA type zeolite, nanoporous, glass, pseudomorphic transformation

1. INTRODUCTION

Porous glasses have many applications as desalination membranes [1], membranes for mixed gas separation, and catalysts [2]. A well-established method to prepare porous glass is called Vycor process, where the porous structure is obtained by acid leaching of a phase separated alkali borosilicate glass [3]. The sol-gel transition of silicon alkoxide polymer solutions is also used for preparation of porous glass [4, 5]. In both methods, the products with wide ranges of pore diameters including micropores (pore diameter $d < 2.0$ nm), mesopores ($2.0 < d < 50$ nm), and macropores ($d > 50$ nm) are obtained [5, 6].

Zeolites are aluminosilicate crystals with micropores. The structure of zeolites is made up of AlO_4 and SiO_4 tetrahedra that are linked to each other forming a three-dimensional framework [7]. By strong acid or heat treatments, zeolite with low Si/Al ratio, such as LTA type zeolite, easily becomes amorphous. Recently, formation of amorphous materials with the morphology of the original zeolite crystals has been reported. Such a phenomenon is known to be noncrystalline pseudomorphism in a field of mineralogy [8]. Cook et al. (1982) obtained noncrystalline pseudomorphs from LTA type zeolite with Na ions (NaA zeolite) by treating it at controlled pH conditions [9]. The heating treatment of partly potassium exchanged NaA zeolite at about 1000 °C for 30 min. also produces noncrystalline pseudomorphs [10]. In both cases, the products were completely amorphous in X-ray diffraction (XRD) with unchanged cubic morphology of LTA type zeolite. However, preservation or formation of pores in the noncrystalline pseudomorph after zeolites has not been characterized in detail.

The formation of mesopores was obtained by dealumination procedures for zeolites with relatively low Si/Al ratio such as zeolite Y [11, 12], LTA type zeolite with Ca ions (CaA zeolite) [13, 14] and NaA zeolite [14]. These were performed either by the hydrothermal treatment of NH_4 exchanged zeolites or by the treatment using ammonium hexafluorosilicate, which are known to remove aluminum from the framework selectively and to improve the stability of zeolite framework. Thus, the resultant products with mesopores usually kept crystalline state.

In the present study, noncrystalline pseudomorph after NaA zeolite was prepared by a combination of acid and hydrothermal treatments. The products were characterized by XRD, Fourier transform-infrared spectroscopy (FT-IR), scanning electron microscopy (SEM) with energy dispersive spectroscopy (EDS), thermogravimetry (TG), and differential thermal analysis (DTA). Porosity of the products was examined by nitrogen adsorption method.

2. EXPERIMENTAL

2.1 Sample preparation

Synthetic NaA zeolite (zeolite A-4, Wako Pure Chemical Industries Ltd.) was used for the starting material. 1.0 g of NaA zeolite was added to 100 mL of 0.06 mol/L HCl solution. The mixture was stirred for 10 minutes at room temperature and filtered through a 0.45 μm membrane with 500 mL of distilled water. During the acid treatment, the pH of the solution was monitored using a pH meter (TOA electronics). A half of the separated solid was dispersed in 60 mL of distilled water and then placed in a Teflon cup fitted into a stainless steel pressure vessel. After heating at 150 °C

for 24 hours, the product was quenched, filtered and dried at 30 °C in an oven for 24 hours.

2.2 Characterization

XRD patterns were obtained with a RINT 2200 (RIGAKU) diffractometer with CuKα radiation. FT-IR spectra were recorded by the diffuse reflectance method using a SPECTRUM 2000 (Parkin-Elmer Ins.). SEM observation was made using a JSM-5800LV (JEOL). EDS analysis was made on five particles for each product using a JED-2110 (JEOL) attached to SEM. The chemical compositions of the products were determined by comparing the intensity of each spectrum of element with that of the starting material (Na/Al = Si/Al = 1 for the starting material). TG and DTA of the products were performed using an Exstar 6000 (SEIKO) from ambient temperature to 1050 °C at a heating rate of 10 °C per minute. Nitrogen adsorption isotherm at -196 °C was measured by the static volumetric system using a BELSORP 28SA (BEL JAPAN, Inc.). Prior to the measurement, the samples were activated at 300 °C under a reduced pressure for 12 hours. Pore-size distribution was deduced from the nitrogen adsorption isotherm by using Dollimore-Heal (D-H) method [15].

3. RESULTS

3.1 XRD

Figure 1 shows the XRD patterns of (a) untreated NaA zeolite, (b) the product after the acid treatment of (a), and (c) the product after the acid and hydrothermal treatment of (b). The XRD pattern of NaA zeolite was typical of LTA type zeolite with no trace of impurity. After the acid treatment, the peak intensities of NaA zeolite became weaker and the amorphous halo around 2θ = 27 degrees increased. These peaks completely disappeared after the subsequent hydrothermal treatment. This indicates that the NaA zeolite was changed to almost amorphous by the acid treatment and completely amorphous by the subsequent hydrothermal treatment.

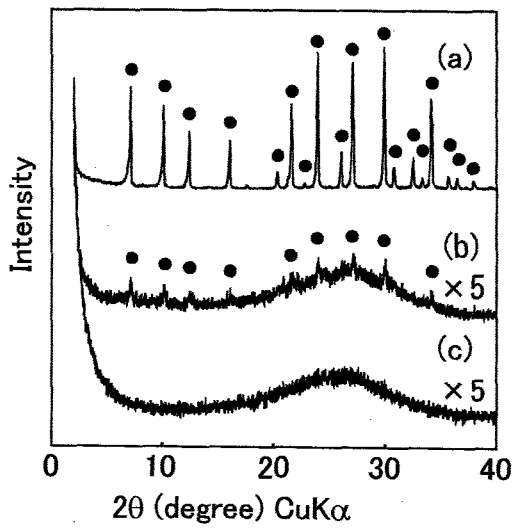

Figure 1. XRD patterns of (a) NaA zeolite, (b) the product after HCl treatment of (a), and (c) the product after hydrothermal treatment of (b).
●: NaA zeolite.

3.2 FT-IR

Figure 2 shows the FT-IR spectra of (a) untreated NaA zeolite, (b) the product after the acid treatment of (a), and (c) the product after the acid and hydrothermal treatment of (b). In the spectrum of untreated NaA zeolite, a sharp band at 560 cm^{-1} due to the external vibration of double 4-rings was observed [16]. Other bands at 995, 660, and 464 cm^{-1} are assigned to the internal vibration of T(Si, Al)-O asymmetric stretching, internal vibration of T-O symmetric stretching, and internal vibration of T-O bending, respectively [16]. These bands were either broadened or disappeared after the acid treatment. The features of IR spectrum of the product after the acid treatment were similar to those reported on the amorphous aluminosilicate gel which is used for the synthesis of NaA zeolite [17]. No significant change was observed between the products before and after the hydrothermal treatment.

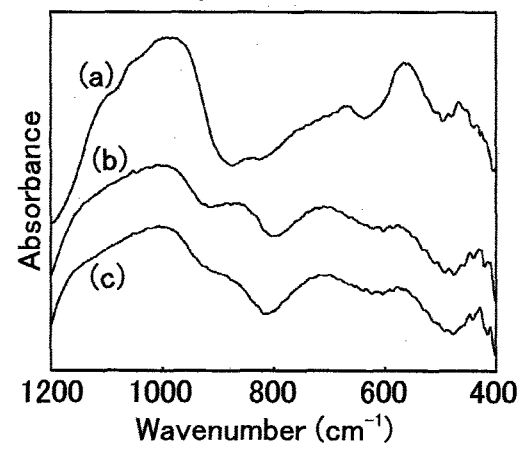

Figure 2. FT-IR spectra of (a) NaA zeolite, (b) the product after HCl treatment of (a), and (c) the product after hydrothermal treatment of (b).

3.3 SEM-EDS

Figure 3 shows the SEM images of (a) untreated NaA zeolite, (b) the product after the acid treatment of (a), and (c) the product after the acid and hydrothermal treatment of (b). The typical cubic morphology of NaA zeolite was retained after the acid and hydrothermal treatments. The chemical compositions by EDS analysis indicated that the Na/Al ratio was remarkably decreased from 1 to 0.19 ± 0.06 by the acid treatment, whereas the Si/Al ratio showed little change (1 to 1.06 ± 0.04). By the treatment, the pH of the solution changed from 1.32 to 4.20 indicating the consumption of H ions. After the subsequent hydrothermal treatment, the Na/Al and Si/Al ratio little changed. These were 0.14 ± 0.06 and 1.01 ±0.05, respectively.

3.4 TG-DTA

TG and DTA curves of untreated NaA zeolite and treated products are shown in Fig. 4. Weight loss by TG analysis for the products was 21.0 % for untreated NaA zeolite, 29.5 % for the product after acid treatment, and 27.1 % for the product after the acid and hydrothermal treatment. This indicates that considerable amount of water was held in the structure after both the acid and hydrothermal treatments. The DTA curve for NaA zeolite was typical one for LTA type zeolite. It showed a

dehydration endotherm peak below 400 °C and two exotherm peaks at 880 and 912 °C corresponding to the amorphization and crystallization of carnegieite, respectively [18]. Up to 400 °C the DTA curve for the product after the acid treatment has a sharp endotherm peak. The peak temperature of dehydration for the product after the acid treatment was lower than that of NaA zeolite. On the other hand, DTA curve for the product after the subsequent hydrothermal treatment have bimodal shape. Both products showed no significant structural change up to 1000 °C where the crystallization of mullite took place as indicated by the exotherm peaks.

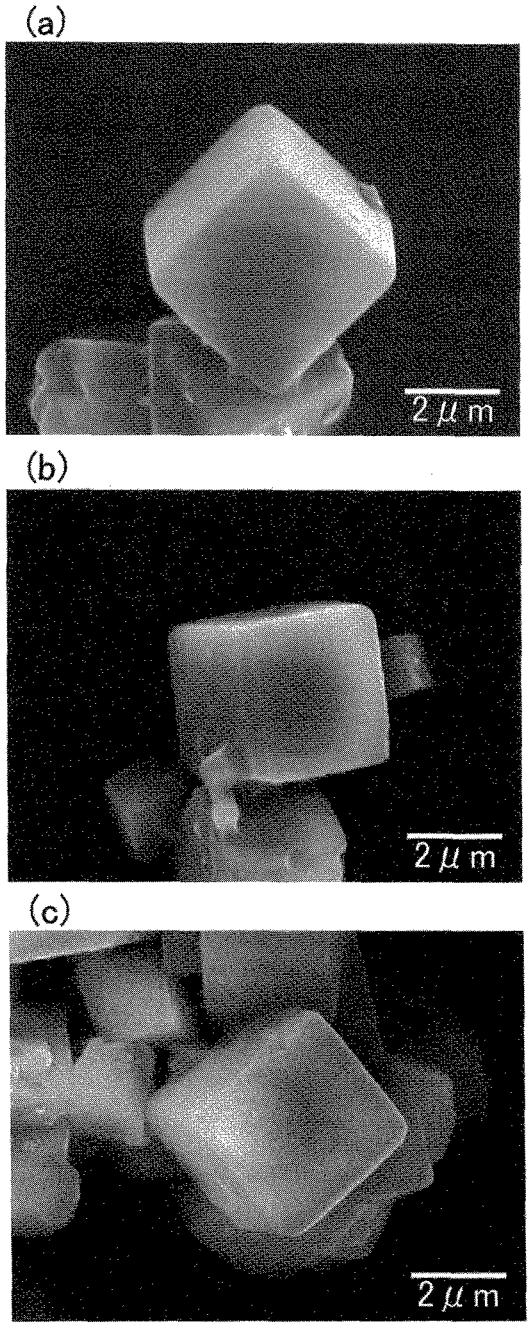

Figure 3. SEM photographs of (a) NaA zeolite, (b) the product after HCl treatment of (a), and (c) the product after hydrothermal treatment of (b).

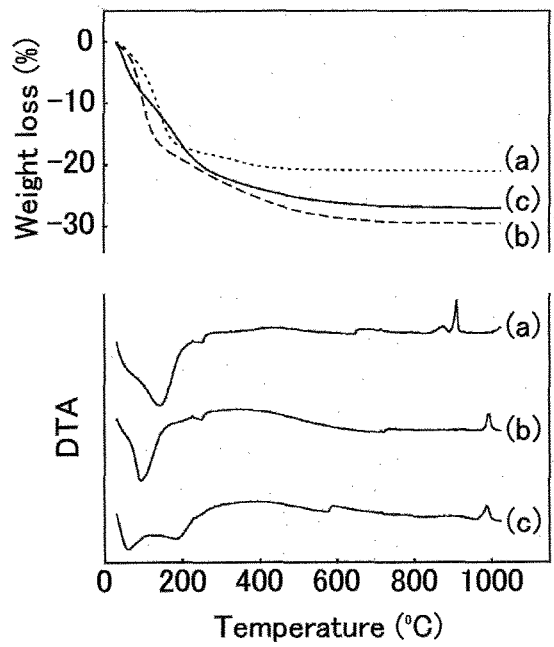

Figure 4. TG (upper) and DTA (lower) curves. (a) NaA zeolite, (b) the product after HCl treatment of (a), and (c) the product after hydrothermal treatment of (b).

3.5 Nitrogen adsorption measurements

Figure 5 shows pore-size distribution of untreated NaA zeolite and the treated products. In the figure, the range of pore diameter including the original pore size of NaA zeolite (about 0.4 nm) is not shown because nitrogen molecules hardly enter the NaA zeolite pores at the present conditions [19]. The pore-size distributions of the NaA zeolite and the product after the acid treatment showed no distinct peak, whereas the product after the acid and hydrothermal treatment showed a sharp peak at 1.9 nm.

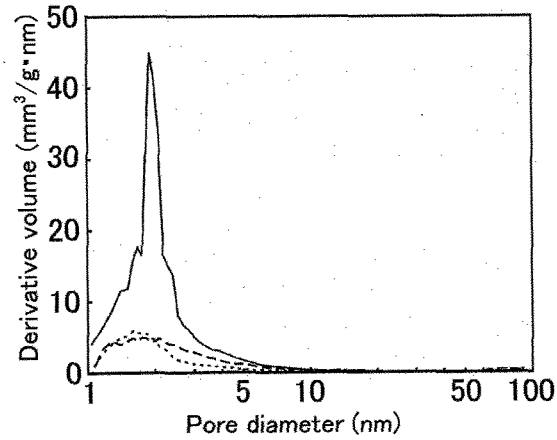

Figure 5. Pore size distributions deduced from the nitrogen adsorption measurements. Dotted line: NaA zeolite. Broken line: the product after HCl treatment of NaA zeolite. Solid line: the product after HCl and hydrothermal treatment.

4. DISCUSSION

The noncrystalline pseudomorph after NaA zeolite,

i.e., the glass with cubic morphology, was obtained after the acid and hydrothermal treatment. The XRD patterns showed that the NaA zeolite was changed to almost amorphous by the acid treatment and completely amorphous by the subsequent hydrothermal treatment. During the acid treatment, a significant decrease of Na and the consumption of H ions were confirmed. Therefore, the following Na-H ion exchange (Eq.1) was the key mechanism for the formation of noncrystalline pseudomorph after NaA zeolite [9].

$$Na_{12}Al_{12}Si_{12}O_{48} + 12H^+ \rightarrow 12Na^+ + H_{12}Al_{12}Si_{12}O_{48} \quad (1)$$

The H ion entered the zeolite structure is considered to interact with the Al-O-Si bond of the framework forming Al-OH-Si [20]. The results by FT-IR suggested that the number of double 4-rings, which are the characteristic building units of LTA type framework, were decreased. Thus, the amorphization would be a result of the reaction of H ions with the framework involving the decomposition of Al-O-Si bonds.

By the subsequent hydrothermal treatment, the transformation of NaA zeolite to noncrystalline pseudomorph was completed. In addition, nitrogen adsorption measurement confirmed the formation of nanopores with mean diameter at 1.9 nm during the subsequent hydrothermal treatment. Dehydration behaviors observed by TG-DTA also supported the presence of pores after the acid and hydrothermal treatments. These are explained by the further decomposition of the framework. It is well known that acid or hydrothermal treatment extracts the Al atoms selectively from the framework of zeolites with relatively high Si/Al ratio [11-14]. In the present study, however, the Si/Al ratio of NaA zeolite was hardly changed by both acid and hydrothermal treatments. Presumably, the attack by acid and hydrothermal reaction resulted in the congruent release of Si and Al for LTA type zeolite having Si/Al = 1 because of the similar configuration of Si and Al atoms in the framework surrounded by four Al-O-Si bonds [7].

Although it was not determined whether or not the original micropores of NaA zeolite remains, the combination of the acid and hydrothermal treatment should be a new method for the formation of porous glass which would be useful for eco-functional materials such as adsorbents, catalysts, ion-exchange media, and membranes.

ACKNOWLEDGEMENTS

We would like to express our sincere gratitude to Dr. T. Kodaira (AIST) and Dr. H. Hashizume (NIMS) for their valuable discussions, and to Mr. S. Awatsu (NIMS) for his help in nitrogen adsorption study.

REFERENCES

[1] T. H. Elmer, *Am. Ceram. Soc. Bull.*, **57**, 1051-53 (1978).
[2] P. W. McMillan, *Phys. Chem. Glasses*, **17**, 193-204 (1976).
[3] T. H. Elmer, M. E. Nordberg, G. B. Carrier and E. J. Korda, *J. Am. Ceram. Soc.*, **53**, 171-75 (1970).
[4] T. Yazawa, *Hyomen (Surface)*, **29**, 971-77 (1991) [in Japanese].
[5] R. Takahashi, K. Nakanishi and N. Soga, *J. Non-Cryst. Solids*, **189**, 66-76 (1995).
[6] H. Tanaka, T. Yazawa, K. Eguchi, H. Nagasawa, N. Matsuda and T. Einishi, *J. Non-Cryst. Solids*, **65**, 301-09 (1985).
[7] D. W. Breck, "Zeolite Molecular Sieves", Wiley, New York, (1974) pp. 45-55.
[8] W. H. Baur, *Microporous Mesoporous Mater.*, **25**, 229-30.
[9] T. E. Cook, W. A. Cilley, A. C. Savitsky and B. H. Wiers, *Environ. Sci. Technol.*, **16**, 345-50 (1982).
[10] C. Kosanović and B. Sbotić, *Microporous Mater.*, **12**, 261-66 (1997).
[11] U. Lohse and M. Mildebrath, *Z. Anorg. Allg. Chem.*, **476**, 126-135 (1981).
[12] H. Horikoshi, S. Kasahara, T. Fukushima, K. Itabashi, T. Okada, O. Terasaki and D. Watanabe, *Nippon Kagaku Kaishi (J. Chem. Soc. Jpn., Chem. Industr. Chem.)*, 398-404 (1989) [in Japanese].
[13] R. Le Van Mao, N. T. C. Vo, B. Sjiariel, L. Lee and G. Denes, *J. Mater. Chem.*, **2**, 595-99 (1992).
[14] R. Le Van Mao, J. A. Lavigne, B. Sjiariel and C. H. Langford, *J. Mater. Chem.*, **3**, 679-83 (1993).
[15] D. Dollimore and G. R. Heal, *J. Appl. Chem.*, **14**, 109-14 (1964).
[16] E. M. Flanigen, H. Khatami and H. A. Szymanski, "Molecular Sieve Zeolites", Ed. by E. M. Flanigen and L. B. Sand, Adv. Chem. Ser., 101, Washington (1971) pp. 201-228.
[17] B. Sbotić, A. M. Tonejc, D. Bagović, A. Čižmek and T. Antonić, *Stud. Surf. Sci. Catal.*, **84**A, 259-66 (1994).
[18] W. Schmitz, H. Siegel and R. Schöllner, *Cryst. Res. Technol.*, **16**, 385-89 (1981).
[19] I. Suzuki, H. Sato, K. Saito and S. Oki, *J. Catal.*, **113**, 540-43 (1988).
[20] D. W. Breck, "Zeolite Molecular Sieves", Wiley, New York, (1974) pp.461.

(Received October 10, 2003; Accepted October 31, 2003)